九州工業大学学術機関リポジトリ

Kyutacar

Kyushu Institute of Technology Academic Repository

GW calculation of plasmon excitations in the quasi-one-dimensional organic compound (TMTSF)2PF6

GW calculation of plasmon excitations in the quasi-one-dimensional organic compound (TMTSF)$_2$PF$_6$

Kazuma Nakamura,[1] Shiro Sakai,[2] Ryotaro Arita,[2] and Kazuhiko Kuroki[3]

[1]*Quantum Physics Section, Kyushu Institute of Technology, 1-1 Sensui-cho, Tobata, Kitakyushu, Fukuoka, 804-8550, Japan*
[2]*Department of Applied Physics, The University of Tokyo, Hongo, Bunkyo-ku, Tokyo 113-8656, Japan*
[3]*Department of Physics, Osaka University, 1-1 Machikaneyama, Toyonaka, Osaka 560-0043, Japan*

We present an *ab initio GW* calculation to study dynamical effects on an organic compound (TMTSF)$_2$PF$_6$. Calculated polarized reflectivities reproduce experimental plasma edges at around 0.2 eV for $E \| b'$ and 1.0 eV for $E \| a$. The low-energy plasmons come out from the low-energy narrow bands energetically isolated from other higher-energy bands, and affect the low-energy electronic structure via the *GW*-type self-energy. Because of the quasi-one-dimensional band structure, a distinct plasmaron state is observed along the Y-Γ line and a large plasmon-induced electron scattering is found in the low-energy occupied states along the X-M line.

I. INTRODUCTION

The physics and chemistry of organic conductors have recently attracted much attention owing to their low dimensionality, strong electron correlation, and material variety and flexibility. Despite the complicated structure of the molecules themselves, the rather simple and energetically isolated band structure commonly seen in these materials provides an ideal basis for studying the fundamental physics of electron correlation. Among a number of organic conductors, (TMTSF)$_2$PF$_6$ has been of particular interest ever since its discovery as the first organic superconductor.[1] In this material, the molecules are stacked along the a axis, and this is the most conductive axis because the molecular orbitals are elongated in the stack direction. A small overlap between neighboring molecular orbitals in the interstack direction gives rise to a weak two dimensionality. The importance of electron correlation can readily be seen from the presence of the spin density wave (SDW) phase, which takes place below 12 K at ambient pressure.[2] The SDW transition temperature decreases upon applying hydrostatic pressure, and superconductivity sits next to the SDW phase in the temperature-pressure phase diagram. The superconducting state also shows some interesting features suggesting unconventional pairing, which may also be a manifestation of electron correlation.[3]

Theoretically, the microscopic origin of the density waves and superconductivity has been intensively investigated on simplified Hubbard-type models where on-site and/or short-ranged off-site repulsions are taken into account.[3] On the other hand, recent *ab initio* studies on organic materials show that the long-range part of the Coulomb interactions is appreciably present,[4,5] suggesting that dielectric properties can also be of interest. In fact, reflectance measurements of (TMTSF)$_2$PF$_6$ show the presence of a plasma edge,[6,7] indeed indicating the importance of the long-range Coulomb interaction.

In general in solids, the energy scale of the plasmon excitation is of the order of 10 eV and therefore it is believed that such excitations are irrelevant to the low-energy physics of the order of 0.1–1 eV. However, in the organic materials, low-energy bands around the Fermi level tend to be isolated from other high-energy bands, resulting in a plasmon characterized by the bandwidth and occupancy of the isolated low-energy bands. Since their bandwidth is typically of the order of ~ 1 eV, the plasma frequency can also be in this energy scale. Then, the plasmon excitation may produce new aspects in the low-energy electronic states through self-energy effects. Since recent progress in angle-resolved photo-emission spectroscopy[8–10] has made it possible to measure quasi-particle band structure and to perform detailed self-energy analyses, corresponding first-principle calculations are highly desired.

In the present study, we present an *ab initio GW* calculation to study dynamical effects on the electronic structure of the organic compound (TMTSF)$_2$PF$_6$. The *GW* calculation takes into account the effect of plasmon excitation.[11–35] The calculated reflectances well reproduce experimental results, identifying the experimentally observed plasma edges to the plasmons within the low-energy bands. By calculating *GW* self-energy and spectral function, we will show that this low-energy plasmon excitation affects the low-energy electronic structure. Since the isolated band character inducing the low-energy plasmon is ubiquitous in strongly correlated electron systems such as organic compounds and transition-metal compounds, the present result will provide a general basis for analyzing various correlated materials.

II. METHOD

Here we describe our scheme. The noninteracting Green's function is given by

$$G_0(\mathbf{r},\mathbf{r}',\omega) = \sum_{\alpha \mathbf{k}} \frac{\psi_{\alpha \mathbf{k}}(\mathbf{r})\psi_{\alpha \mathbf{k}}^*(\mathbf{r}')}{\omega - \epsilon_{\alpha \mathbf{k}} + i\delta\,\mathrm{sgn}(\epsilon_{\alpha \mathbf{k}} - \epsilon_f)}, \quad (1)$$

where $\psi_{\alpha \mathbf{k}}(\mathbf{r})$ and $\epsilon_{\alpha \mathbf{k}}$ are the Kohn-Sham (KS) wave function and its eigenvalue of band α and wave vector $\mathbf{k}$, and ϵ_f is the Fermi level. δ is chosen to be a small but finite positive value to stabilize numerical calculations. A polarization function of a type $-iG_0G_0$ is written in matrix form in the plane-wave

basis as

$$
\chi_{\mathbf{GG'}}(\mathbf{q},\omega)
$$
$$
= 2 \sum_{\mathbf{k}} \sum_{\alpha}^{\text{vir}} \sum_{\beta}^{\text{occ}} M_{\alpha\beta}^{\mathbf{G}}(\mathbf{k},\mathbf{q}) M_{\alpha\beta}^{\mathbf{G'}}(\mathbf{k},\mathbf{q})^*
$$
$$
\times \left\{ \frac{1}{\omega - \epsilon_{\alpha\mathbf{k}+\mathbf{q}} + \epsilon_{\beta\mathbf{k}} + i\delta} - \frac{1}{\omega + \epsilon_{\alpha\mathbf{k}+\mathbf{q}} - \epsilon_{\beta\mathbf{k}} - i\delta} \right\}
$$
$$(2)$$

with $M_{\alpha\beta}^{\mathbf{G}}(\mathbf{k},\mathbf{q}) = \langle \psi_{\alpha\mathbf{k}+\mathbf{q}} | e^{i(\mathbf{q}+\mathbf{G})\mathbf{r}} | \psi_{\beta\mathbf{k}} \rangle$.

Optical properties in a metal are related to the symmetric dielectric function[12] in the $\mathbf{q} \to 0$ limit

$$
\epsilon_{\mathbf{GG'}}(\omega) = \delta_{\mathbf{GG'}} - \frac{(\omega_{pl,\mu\mu})^2}{\omega(\omega + i\delta)} \delta_{\mathbf{G0}} \delta_{\mathbf{G'0}}
$$
$$
- \lim_{\mathbf{q} \to 0} \frac{4\pi}{N\Omega} \frac{\chi_{\mathbf{GG'}}^{\text{inter}}(\mathbf{q},\omega)}{|\mathbf{q}+\mathbf{G}||\mathbf{q}+\mathbf{G'}|}
$$
$$(3)$$

with $\mathbf{q}$ approaching zero along the Cartesian μ direction. N is the total number of sampling k points and Ω is the unit-cell volume. The second term is the Drude term due to the intraband transition around the Fermi level. The third term represents the interband contribution, where $\chi_{\mathbf{GG'}}^{\text{inter}}(\mathbf{q},\omega)$ is a polarization matrix due to the interband transitions. Plasma frequency in the second term is given in a tensor form by[36,37]

$$
\omega_{pl,\mu\nu} = \sqrt{\frac{8\pi}{\Omega N} \sum_{\alpha\mathbf{k}} p_{\alpha\mathbf{k},\mu} p_{\alpha\mathbf{k},\nu} \delta(\epsilon_{\alpha\mathbf{k}} - \epsilon_f)}
$$
$$(4)$$

with $p_{\alpha\mathbf{k},\mu}$ being a matrix element of a momentum as

$$
p_{\alpha\mathbf{k},\mu} = -i \langle \psi_{\alpha\mathbf{k}} | \frac{\partial}{\partial x_\mu} + [V_{NL}, x_\mu] | \psi_{\alpha\mathbf{k}} \rangle,
$$
$$(5)$$

where V_{NL} is the nonlocal part of the pseudopotential.

The GW self-energy is given by

$$
\Sigma(\mathbf{r},\mathbf{r}',\omega) = i \int \frac{d\omega'}{2\pi} G_0(\mathbf{r},\mathbf{r}',\omega + \omega') W(\mathbf{r},\mathbf{r}',\omega') e^{i\eta\omega'},
$$
$$(6)$$

where the number η is positive infinitesimal. The screened Coulomb interaction $W(\omega) = v^{1/2} \epsilon^{-1}(\omega) v^{1/2}$ is decomposed into the bare Coulomb interaction v and the frequency-dependent part $W_C(\omega) = W(\omega) - v$. The ϵ^{-1} is given by the inverse of the matrix in the reciprocal space

$$
\epsilon_{\mathbf{GG'}}(\mathbf{q},\omega) = \delta_{\mathbf{GG'}} - \frac{4\pi}{N\Omega} \frac{1}{|\mathbf{q}+\mathbf{G}|} \chi_{\mathbf{GG'}}(\mathbf{q},\omega) \frac{1}{|\mathbf{q}+\mathbf{G'}|},
$$

and incorporates the local-field effect. Since ϵ^{-1} thus defined contains an infinite series of the polarizations coupled by the bare Coulomb interaction, it can describe a collective charge excitation (plasmon). The frequency integral of $iG_0 v$ gives the bare exchange term Σ_X and that of $iG_0 W_C$ gives the correlation term $\Sigma_C(\omega)$ including the retardation effect. The calculation of Σ_X is straightforward while that of $\Sigma_C(\omega)$ is somewhat technical. In the present calculation, we fit the following function to *ab initio* $W_C(\omega)$:[35]

$$
\tilde{W}_C(\mathbf{r},\mathbf{r}',\omega) = \sum_j \left(\frac{1}{\omega - z_j} + \frac{1}{\omega + z_j} \right) a_j(\mathbf{r},\mathbf{r}'),
$$
$$(7)$$

where z_j and $a_j(\mathbf{r},\mathbf{r}')$ are the pole and amplitude of the model interactions, respectively. Since the frequency-dependent part

is decoupled from the amplitude in $\tilde{W}_C$, the frequency integral in $iG_0\tilde{W}_C$ can be analytically performed. The resulting matrix elements of $\Sigma_C(\omega)$ are

$$
\langle \psi_{\alpha\mathbf{k}} | \Sigma_C(\omega) | \psi_{\alpha\mathbf{k}} \rangle
$$
$$
= \sum_{jn\mathbf{q}} \frac{\langle \psi_{\alpha\mathbf{k}} \psi_{n\mathbf{k}-\mathbf{q}} | a_j | \psi_{n\mathbf{k}-\mathbf{q}} \psi_{\alpha\mathbf{k}} \rangle}{\omega - \epsilon_{n\mathbf{k}-\mathbf{q}} - (z_j - i\delta)\text{sgn}(\epsilon_{n\mathbf{k}-\mathbf{q}} - \epsilon_f)}.
$$
$$(8)$$

The spectral function is calculated by

$$
A(\mathbf{k},\omega) = \frac{1}{\pi} \sum_{\alpha} \left| \text{Im} \frac{1}{\omega - (\epsilon_{\alpha\mathbf{k}} + \Delta\Sigma_{\alpha\mathbf{k}}(\omega) + \Delta)} \right|,
$$
$$(9)$$

where $\Delta\Sigma_{\alpha\mathbf{k}}(\omega) = \langle \psi_{\alpha\mathbf{k}} | \Sigma(\mathbf{r},\mathbf{r}',\omega) - v_{XC}(\mathbf{r})\delta(\mathbf{r} - \mathbf{r}') | \psi_{\alpha\mathbf{k}} \rangle$, and v_{XC} is the exchange-correlation potential. A shift Δ is introduced to keep the electron density the same as that of KS, N_{elec}, i.e., $\int_{-\infty}^{\epsilon_f} d\omega \int d\mathbf{k} \, A(\mathbf{k},\omega) = N_{\text{elec}}$.

III. RESULTS AND DISCUSSIONS

Our density-functional calculations are based on the Tokyo *Ab Initio* Program Package (TAPP) (Ref. 38) with plane-wave basis sets, where we employ norm-conserving pseudopotentials[39,40] and generalized gradient approximation (GGA) for the exchange-correlation potential.[41] The experimental structure of $(TMTSF)_2PF_6$ obtained by a neutron measurement[42] at 20 K is adopted. The cutoff energies in wave function and in charge densities are 36 and 144 Ry, respectively, and an $11 \times 11 \times 3$ k-point sampling is employed. The maximally localized Wannier function (MLWF) (Refs. 43 and 44) is used for interpolation of the self-energy and spectral function to a finer k grid. The cutoff of polarization function is set to be 3 Ry and 198 bands are considered, which cover an energy range from the bottom of the occupied states near -30 eV to the top of the unoccupied states near 15 eV. The integral over the Brillouin zone (BZ) is evaluated by the generalized tetrahedron method.[35,45] The polarization up to $\omega = 86$ eV is calculated in a logarithmic mesh with 110 energy points. The frequency dependence of the self-energy for the states near the Fermi level is calculated for $[-30\text{ eV}: 30\text{ eV}]$ with an interval of 0.01 eV. The broadening δ in Eqs. (2), (3), and (8) is set to 0.02 eV. The shift Δ in the spectral function $A(\mathbf{k},\omega)$ in Eq. (9) is found to be 0.96 eV. The self-energy at $\mathbf{q} = \mathbf{G} = 0$ is treated in the manner in Ref. 46.

Figure 1(a) shows the calculated GGA band structure of $(TMTSF)_2PF_6$. We find two narrow bands around the Fermi level, which are well separated in energy from other higher-energy bands. The appearance of such isolated low-energy bands is common to various organic conductors.[4,5,47–51] We assign these bands to "target bands" for which the self-energy effects are considered below. We construct MLWFs for the target bands and evaluate the transfer integrals as shown in panel (b). The transfer integrals well reproduce the original bands as shown by the blue-dotted curves in panel (a). Note that the transfers along the a axis are about four times larger than those along the b axis, reflecting a quasi-one-dimensional structure of the compound.

Figure 2(a) shows the calculated energy loss function $-\text{Im}\,\epsilon^{-1}(\omega)$. The red-solid and green-dotted curves are results for the light polarization E parallel to a (along the x axis) and
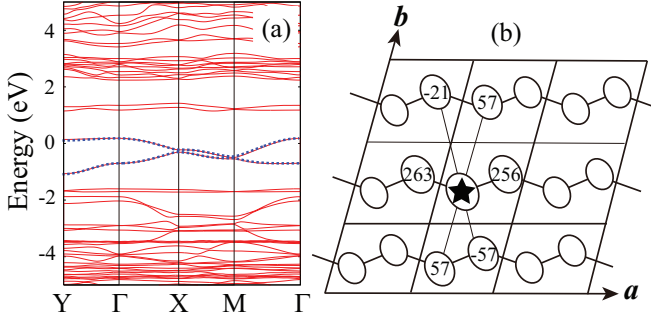
FIG. 1. (Color online) (a) GGA band structure of $(TMTSF)_2PF_6$, along the high-symmetry lines in the ab plane, where $\Gamma = (0,0,0)$, $X = (a^*/2,0,0)$, $M = (a^*/2,b^*/2,0)$, and $Y = (0,b^*/2,0)$. The Fermi level is at zero energy. (b) Schematic crystal structure in the ab plane, where the unit cell contains two TMTSF molecules denoted by the ellipsoids. The number in the ellipsoids represents the transfer integral (in the unit of meV) between the highest-occupied molecular orbitals at the starred site and each site. The tight-binding bands [blue dotted curves in panel (a)] are calculated from these transfers.

b' (along the y axis), respectively. In the low-energy region, we find two plasmon peaks: one at ~0.2 eV for $E\|b'$ and the other at ~1.0 eV for $E\|a$. These peaks result from the plasmon excitations within the isolated target bands which have a low carrier density and small bandwidths. These plasmons are distinct from the plasmon seen at around 20 eV, which is relevant to the total charge density and the bare electron mass. We note that the difference between the plasmon peaks for
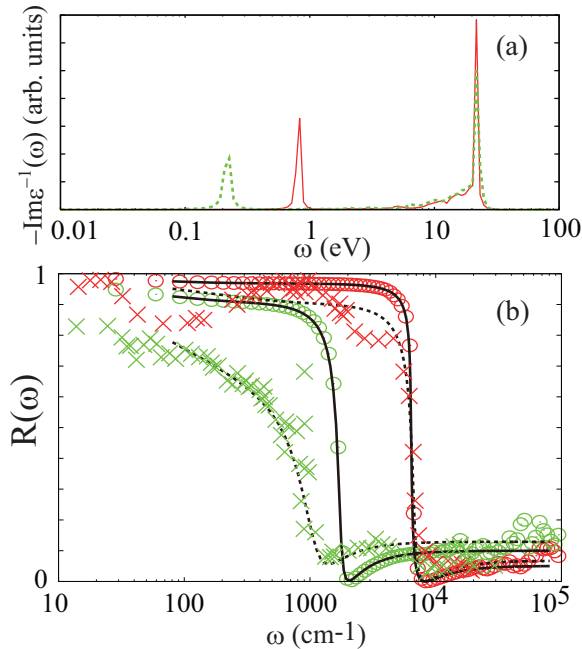

FIG. 2. (Color online) (a) Calculated energy loss function of $(TMTSF)_2PF_6$. The red-solid and green-dotted curves represent the spectra for $E\|a$ and $E\|b'$, respectively. (b) *Ab initio* reflectivity (circles) and experimental one (crosses) at 25 K (Ref. 7). The results for $E\|a$ and $E\|b'$ are displayed by dark red and light green, respectively. The solid and dotted curves are the fits by Eq. (11) with parameters shown in Table I.

TABLE I. Comparison of Drude-model parameters in Eq. (11) for $(TMTSF)_2PF_6$ between theory and experiment of Ref. 7. The unit of the plasma frequency is cm^{-1}.

	$E\|a$		$E\|b'$	
	ϵ_{core}	ω_{pl}	ϵ_{core}	ω_{pl}
Theory	2.5	10 074	3.7	3331
Expt.	2.9	11 400	4.5	2360

$E\|a$ and $E\|b'$ reflects the difference in the transfer integrals (~ 260 meV along the a axis and ~ 60 meV along the b axis). Also note that the low-energy plasmon spectra are rather sharp, reflecting the small energy scale of the isolated narrow low-energy bands where the low-energy plasmons are formed. The spectral width is also sensitive to the broadening factor δ introduced in the Green's function in Eq. (1), though δ does not essentially change the plasma frequency.

Figure 2(b) compares the reflectance

$$R_{\mu\mu}(\omega) = \left| \frac{1 - \sqrt{\epsilon_{\mu\mu}^{-1}(\omega)}}{1 + \sqrt{\epsilon_{\mu\mu}^{-1}(\omega)}} \right| \qquad (10)$$

between our theory (circles) and the experiment (crosses) of Ref. 7. The calculated result reproduces the experimental one fairly well, in particular, for $E\|a$ (dark red). The smaller energy scale of $E\|b'$ (light green) is also qualitatively reproduced.

To quantify the comparison, we fit the following function to theoretical and experimental reflectance data:

$$\epsilon_{\mu\mu}(\omega) = \epsilon_{core,\mu\mu} - \frac{\omega_{pl,\mu\mu}^2}{\omega(\omega + i\delta)}. \qquad (11)$$

For the theoretical data, $\omega_{pl,\mu\mu}$ is calculated with Eq. (4) and δ is fixed at 0.02 eV, so that the effective dielectric constant $\epsilon_{core,\mu\mu}$ is the only free parameter in the fitting. Table I summarizes the values of $\epsilon_{core,\mu\mu}$ and $\omega_{pl,\mu\mu}$. The calculated results well reproduce the experimental ones,[52] although the theoretical plasma edge of $E\|b'$ is by ~1.5 times higher than that of experiment.

The low-energy plasmons found in Fig. 2 can affect the low-energy electronic structure. To see this effect, we show in Fig. 3(a) the *GW* spectral function $A(\mathbf{k},\omega)$ [Eq. (9)]. While the quasiparticle band structure around -1.0–0.1 eV is similar
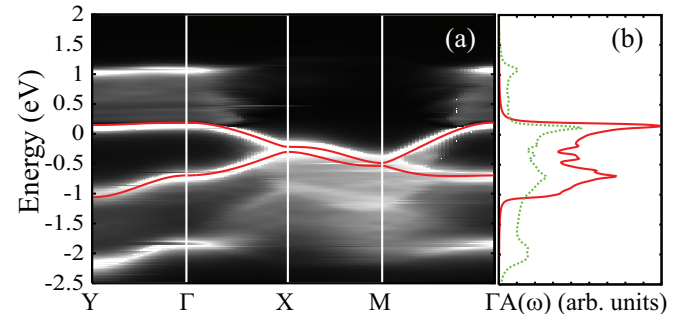

FIG. 3. (Color online) (a) Calculated spectral function $A(\mathbf{k},\omega)$ of $(TMTSF)_2PF_6$, superposed by the Kohn-Sham band structure (red curves). The Fermi level is at zero energy. (b) Density of states obtained by KS (red-solid curve) and *GW* (green-dotted curve).
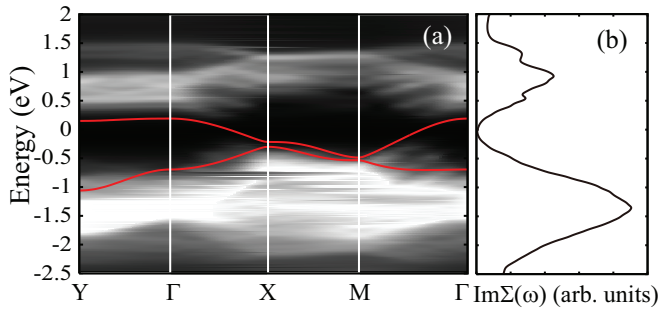
FIG. 4. (Color online) Calculated spectrum of (a) Im $\Sigma(\mathbf{k},\omega)$ and (b) Im $\Sigma(\omega)$ of $(TMTSF)_2PF_6$. The Fermi level is at zero energy. The Kohn-Sham band structure (red solid curves) is superposed in panel (a).

to that of KS (red solid curves), we see an appreciable weight transfer to higher energy due to the self-energy effects. Along the Y-Γ line, new states emerge about 1 eV above (below) the unoccupied (occupied) part of the low-energy narrow bands. Along the X-M line, the spectra are more broadened and spread in the range from -1.5 to 0 eV. In panel (b), the density of states calculated by KS (red-solid curve) and by GW (green-dotted curve) is displayed, from which we see that a considerable amount of weight is transferred to higher energy due to the self-energy effect.

To get insight into the relation between the dielectric function (Fig. 2) and the spectral function (Fig. 3), we plot in Fig. 4 Im $\Sigma(\mathbf{k},\omega) = \sum_\alpha |\text{Im} \Sigma_{\alpha\mathbf{k}}(\omega)|$ [(a)] and Im $\Sigma(\omega) = \int d\mathbf{k} \, \text{Im} \, \Sigma(\mathbf{k},\omega)$ [(b)]. Im $\Sigma(\mathbf{k},\omega)$ is directly related to the dielectric function through Eq. (6), and to the spectral function through Eq. (9). We see that Im $\Sigma(\mathbf{k},\omega)$ has strong intensities at 0.5–1.0 eV and -2.0 to -0.5 eV; about 0.5 eV above (below) the unoccupied (occupied) part of the low-energy bands. The energy scale of 0.5 eV roughly corresponds to the average of $\omega_{pl,b'} \sim 0.2$ eV and $\omega_{pl,a} \sim 1.0$ eV. Since the plasmons are known to make a peak in Im Σ at energy $\epsilon_{unocc} + \omega_{pl}$ or $\epsilon_{occ} - \omega_{pl}$,[14] the bright region in Fig. 4(a) can be interpreted as an effect of the low-energy plasmons in Fig. 2, although the electron-electron scattering other than the plasmon excitation can also contribute to Im $\Sigma(\mathbf{k},\omega)$. Since the strong peak of Im $\Sigma(\mathbf{k},\omega)$ causes a large variation of Re $\Sigma(\mathbf{k},\omega)$ through the Kramers-Kronig

relation, new poles of the Green's function can be created just outside of the peak of Im $\Sigma(\mathbf{k},\omega)$. The new states emerging in $A(\mathbf{k},\omega)$ in Fig. 3 are reminiscent of a plasmaron,[53,54] which is a coupled mode of the elementary charges and plasmons. Here the plasmaron has an unusually low energy, reflecting the character of the isolated-narrow low-energy bands. Experimental observation of such a low-energy plasmaron in the present organic compound or in other materials like transition-metal oxides, which often have isolated low-energy bands, is an interesting future issue.

IV. CONCLUSION

In summary, we study low-energy dynamical properties of an organic compound $(TMTSF)_2PF_6$ from first principles. Theoretical reflectance reproduces experimentally observed plasma edges, and their anisotropy due to the quasi-one-dimensional nature. The low-energy plasmons come out from the energetically isolated bands around the Fermi level. The self-energy effect due to these plasmon excitations on the low-energy electronic structure is studied within the GW approximation. We have found that the self-energy effect is appreciable at energy by ~ 0.5 eV above (below) the unoccupied (occupied) part of the low-energy bands, suggesting that the plasmons can influence low-energy physics as the formation of the plasmaron state, i.e., a quasiparticle combined with a plasmon. Since organic conductors, or more generally, strongly correlated electron materials, often have such isolated bands around the Fermi level, we expect that similar low-energy plasmon excitation can be relevant to physical properties of these materials. A detection of these effects in experiments such as photoemission spectroscopy is an interesting future issue.

[1]D. Jerome, A. Mazaud, M. Ribault, and K. Bechgaard, J. Phys. Lett. (Paris) **41**, L95 (1980).

[2]For a review, see, e.g, T. Ishiguro, K. Yamaji, and G. Saito, *Organic Superconductors* (Springer-Verlag, Heidelberg, 1998).

[3]For a review, see, e.g, K. Kuroki, J. Phys. Soc. Jpn. **75**, 051013 (2006).

[4]K. Nakamura, Y. Yoshimoto, T. Kosugi, R. Arita, and M. Imada, J. Phys. Soc. Jpn. **78**, 083710 (2009).

[5]K. Nakamura, Y. Yoshimoto, and M. Imada, Phys. Rev. B **86**, 205117 (2012).

[6]Martin Dressel, ISRN Condensed Matter Physics **2012**, 732973 (2012).

[7]C. S. Jacobsen, D. B. Tanner, and K. Bechgaard, Phys. Rev. Lett. **46**, 1142 (1981).

[8]T. Kiss, A. Chainani, H. M. Yamamoto, T. Miyazaki, T. Akimoto, T. Shimojima, K. Ishizaka, S. Watanabe, C.-T. Chen, A. Fukaya, R. Kato, and S. Shin, Nat. Commun. **3**, 1089 (2012).

[9]F. Zwick, S. Brown, G. Margaritondo, C. Merlic, M. Onellion, J. Voit, and M. Grioni, Phys. Rev. Lett. **79**, 3982 (1997).

[10]R. Claessen, M. Sing, U. Schwingenschlögl, P. Blaha, M. Dressel, and C. S. Jacobsen, Phys. Rev. Lett. **88**, 096402 (2002).

[11]L. Hedin, Phys. Rev. **139**, A796 (1965).

[12]M. S. Hybertsen and S. G. Louie, Phys. Rev. B **34**, 5390 (1986).

[13] G. Onida, L. Reining, and A. Rubio, Rev. Mod. Phys. **74**, 601 (2002).

[14] F. Aryasetiawan and O. Gunnarsson, Rep. Prog. Phys. **61**, 237 (1998).

[15] M. S. Hybertsen and S. G. Louie, Phys. Rev. Lett. **55**, 1418 (1985).

[16] R. W. Godby, M. Schlüter, and L. J. Sham, Phys. Rev. Lett. **56**, 2415 (1986).

[17] R. W. Godby, M. Schlüter, and L. J. Sham, Phys. Rev. B **35**, 4170 (1987).

[18] J. E. Northrup, M. S. Hybertsen, and S. G. Louie, Phys. Rev. Lett. **59**, 819 (1987).

[19] N. Hamada, M. Hwang, and A. J. Freeman, Phys. Rev. B **41**, 3620 (1990).

[20] F. Aryasetiawan, Phys. Rev. B **46**, 13051 (1992).

[21] F. Aryasetiawan and O. Gunnarsson, Phys. Rev. Lett. **74**, 3221 (1995).

[22] W. G. Aulbur, L. Joensson, and J. W. Wilkins, Solid State Phys. **54**, 1 (2000).

[23] B. Arnaud and M. Alouani, Phys. Rev. B **62**, 4464 (2000).

[24] W. Ku and A. G. Eguiluz, Phys. Rev. Lett. **89**, 126401 (2002).

[25] M. Usuda, N. Hamada, T. Kotani, and M. van Schilfgaarde, Phys. Rev. B **66**, 125101 (2002).

[26] T. Kotani and M. van Schilfgaarde, Solid State Commun. **121**, 461 (2002).

[27] A. Yamasaki and T. Fujiwara, Phys. Rev. B **66**, 245108 (2002).

[28] S. Lebègue, B. Arnaud, M. Alouani, and P. E. Bloechl, Phys. Rev. B **67**, 155208 (2003).

[29] S. V. Faleev, M. van Schilfgaarde, and T. Kotani, Phys. Rev. Lett. **93**, 126406 (2004).

[30] M. Shishkin and G. Kresse, Phys. Rev. B **74**, 035101 (2006).

[31] T. Kotani, M. van Schilfgaarde, and S. V. Faleev, Phys. Rev. B **76**, 165106 (2007).

[32] C. Friedrich, S. Blügel, and A. Schindlmayr, Phys. Rev. B **81**, 125102 (2010).

[33] R. Sakuma, T. Miyake, and F. Aryasetiawan, Phys. Rev. B **86**, 245126 (2012).

[34] T. Miyake, C. Martins, R. Sakuma, and F. Aryasetiawan, Phys. Rev. B **87**, 115110 (2013).

[35] Y. Nohara, S. Yamamoto, and Takeo Fujiwara, Phys. Rev. B **79**, 195110 (2009).

[36] P. Puschnig and C. Ambrosch-Draxl, Phys. Rev. B **66**, 165105 (2002).

[37] C. Ambrosch-Draxl and J. O. Sofo, Comput. Phys. Commun. **175**, 1 (2006).

[38] J. Yamauchi, M. Tsukada, S. Watanabe, and O. Sugino, Phys. Rev. B **54**, 5586 (1996).

[39] N. Troullier and J. L. Martins, Phys. Rev. B **43**, 1993 (1991).

[40] L. Kleinman and D. M. Bylander, Phys. Rev. Lett. **48**, 1425 (1982).

[41] J. P. Perdew, K. Burke, and M. Ernzerhof, Phys. Rev. Lett. **77**, 3865 (1996).

[42] B. Gallois, J. Gaultier, C. Hauw, T.-d. Lamcharfi, and A. Filhol, Acta Crystallogr., Sect. B: Struct. Sci. **B42**, 564 (1986).

[43] N. Marzari and D. Vanderbilt, Phys. Rev. B **56**, 12847 (1997).

[44] I. Souza, N. Marzari, and D. Vanderbilt, Phys. Rev. B **65**, 035109 (2001).

[45] T. Fujiwara, S. Yamamoto, and Y. Ishii, J. Phys. Soc. Jpn. **72**, 777 (2003).

[46] J. Spencer and A. Alavi, Phys. Rev. B **77**, 193110 (2008).

[47] Y.-N. Xu, W. Y. Ching, Y. C. Jean, and Y. Lou, Phys. Rev. B **52**, 12946 (1995).

[48] W. Y. Ching, Y.-N. Xu, Y. C. Jean, and Y. Lou, Phys. Rev. B **55**, 2780 (1997).

[49] T. Miyazaki and H. Kino, Phys. Rev. B **68**, 220511(R) (2003).

[50] S. Ishibashi and M. Kohyama, Phys. Rev. B **62**, 7839 (2000).

[51] S. Ishibashi, T. Tamura, M. Kohyama, and K. Terakura, J. Phys. Soc. Jpn. **75**, 015005 (2006).

[52] The value of experimental δ at 25 K is 0.071 eV for $E\|a$ and 0.074 eV for $E\|b'$, which seems to be highly temperature dependent (Ref. 7).

[53] B. I. Lundqvist, Phys. Kondens. Mater. **6**, 193 (1967).

[54] D. C. Langreth, Phys. Rev. B **1**, 471 (1970).